JVI Journals.ASM.org

Molecular Determinants of Hepatitis B and D Virus Entry Restriction in Mouse Sodium Taurocholate Cotransporting Polypeptide

Huan Yan,[a,b] Bo Peng,[a] Wenhui He,[a,c] Guocai Zhong,[a] Yonghe Qi,[a,d] Bijie Ren,[a] Zhenchao Gao,[a,b] Zhiyi Jing,[a] Mei Song,[a,c] Guangwei Xu,[a] Jianhua Sui,[a] Wenhui Li[a]

National Institute of Biological Sciences, Beijing, China[a]; Graduate Program in the School of Life Sciences, Peking University, Beijing, China[b]; Graduate Program in the Chinese Academy of Medical Sciences and Peking Union Medical College, Beijing, China[c]; Graduate Program in the School of Life Sciences, Beijing Normal University, Beijing, China[d]

Human hepatitis B virus (HBV) and its satellite virus, hepatitis D virus (HDV), primarily infect humans, chimpanzees, or tree shrews (*Tupaia belangeri*). Viral infections in other species are known to be mainly restricted at the entry level since viral replication can be achieved in the cells by transfection of the viral genome. Sodium taurocholate cotransporting polypeptide (NTCP) is a functional receptor for HBV and HDV, and amino acids 157 to 165 of NTCP are critical for viral entry and likely limit viral infection of macaques. However, the molecular determinants for viral entry restriction in mouse NTCP (mNTCP) remain unclear. In this study, mNTCP was found to be unable to support either HBV or HDV infection, although it can bind to pre-S1 of HBV L protein and is functional in transporting substrate taurocholate; comprehensive swapping and point mutations of human NTCP (hNTCP) and mNTCP revealed molecular determinants restricting mNTCP for viral entry of HBV and HDV. Remarkably, when mNTCP residues 84 to 87 were substituted by human counterparts, mNTCP can effectively support viral infections. In addition, a number of cell lines, regardless of their species or tissue origin, supported HDV infection when transfected with hNTCP or mNTCP with residues 84 to 87 replaced by human counterparts, highlighting the central role of NTCP for viral infections mediated by HBV envelope proteins. These studies advance our understanding of NTCP-mediated viral entry of HBV and HDV and have important implications for developing the mouse model for their infections.

Hepatitis B virus (HBV) is the prototype of the *Hepadnaviridae* (hepatotropic DNA viruses) family (1). Human HBV has infected 2 billion people worldwide, and 350 million of them are chronically infected (2). About two-thirds of hepatocellular carcinoma (HCC) is due to chronic HBV infection (3). Hepatitis D virus (HDV) is a satellite virus of HBV, 15 million people are infected by HDV, and no specific anti-HDV drug is clinically available at present. Chronic HBV patients coinfected with HDV are at high risk for more severe symptoms and more rapid progression (4).

HBV is a small enveloped virus with a relaxed circular partially double-stranded DNA genome of ~3.2 kb encoding four overlapped open reading frames. HBV large (L), middle (M), and small (S) envelope proteins are encoded by a single open reading frame (5). They are translated from different initial codons but share an end. HDV contains a single-stranded, circular RNA genome of ~1,700 nucleotides, with one coding region for small and large form of delta antigens. It replicates in the nucleus and accumulates a large number of viral RNAs and delta antigen (6). Since HDV has to employ HBV envelope proteins for the infection of hepatocytes (7), the entry of HDV is believed to be similar to that of HBV and has been used as a surrogate to study the early entry process (4, 8, 9).

The lack of a convenient *in vitro* viral infection system has been a long-standing hurdle for studying viral entry of HBV and HDV (10). Recently, we identified sodium taurocholate cotransporting polypeptide (NTCP) as a functional receptor for both HBV and HDV (11). Tupaia NTCP also functions as an efficient receptor for woolly monkey HBV (12). NTCP (*Slc10a1*) is a hepatic Na^+-bile acid symporter and is responsible for the vast majority of sodium-dependent uptake of bile salts from enterohepatic circulation (13, 14). Consistent with HBV and HDV liver tropism, NTCP is mainly expressed in hepatocytes and localized to the sinusoidal plasma membrane (15, 16). Exogenous expression of NTCP renders human hepatocellular carcinoma cell line, HepG2, susceptible to the viral infections, thereby providing an easily accessible infection system for HBV and HDV studies and for developing new antiviral drugs.

Human HBV and HDV can infect humans, chimpanzees, and a remote related species of tree shrew (*Tupaia belangeri*) (17–20). Notably, primates that are closely related to *Homo sapiens*, such as Old World monkey baboons and New World monkey tamarins, are not susceptible to HBV infection (8). The host range restriction of HBV and HDV seems to be largely at the entry level since viral replication can be achieved in other species once the entry is bypassed (8, 21–23). NTCP is functionally conserved in mammalians, but protein sequences of NTCP vary among species. We previously reported that crab-eating monkey (*Macaca fascicularis*) NTCP (mkNTCP) neither supports pre-S1 lipopeptide binding nor viral infection of HBV and HDV; however, substituting amino acids (aa) 157 to 165 of mkNTCP with the corresponding hNTCP residues converted mkNTCP to a functional receptor for pre-S1 binding, as well as viral infections (11).

In the present study, we investigated the molecular determinants of mouse NTCP (mNTCP) that restrict viral entry of HBV

Received 1 March 2013 **Accepted** 29 April 2013
Published ahead of print 15 May 2013
Address correspondence to Wenhui Li, liwenhui@nibs.ac.cn.
H.Y. and B.P. contributed equally to this article.

doi:10.1128/JVI.03540-12

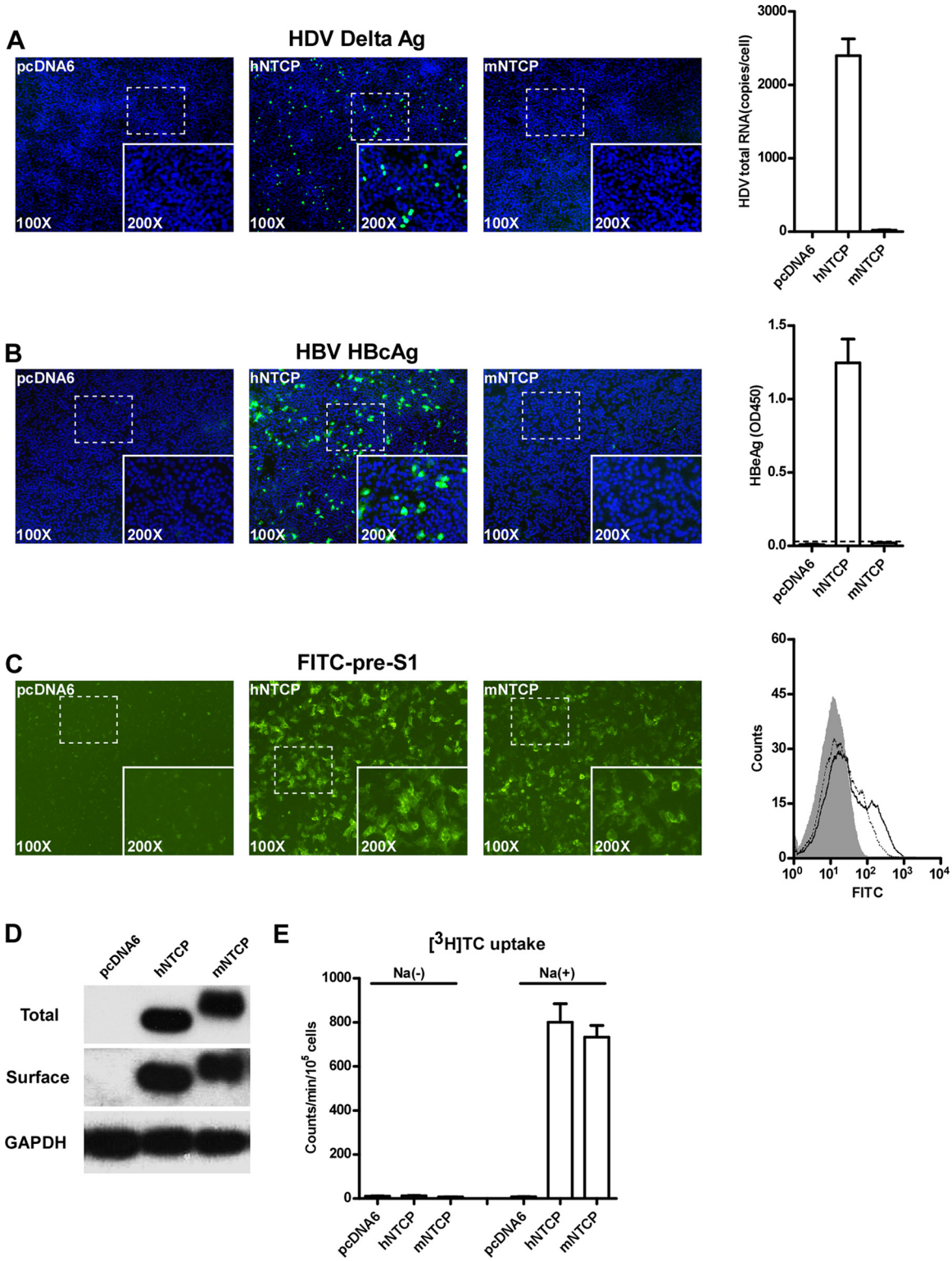

FIG 1 mNTCP does not support HBV and HDV infection but is capable of pre-S1 binding. (A) HepG2 cells were transfected with human or mouse NTCP or a pcDNA6 vector control. Transfected cells were maintained in PMM for 24 h and then inoculated with 500 multiplicities of genome equivalents (mge) of HDV in the presence of 5% PEG8000. Intracellular HDV delta antigen, mainly in the nucleus, was detected by FITC-conjugated MAb 4G5 at 8 days postinfection (dpi). Cell nuclei were stained with DAPI in blue (left). HDV RNA copy numbers were measured by real-time reverse transcription-PCR (RT-PCR) and presented as HDV RNA copies per cell (right). (B) HepG2 cells were transfected as in panel A and infected with 100 mge of HBV in the presence of 5% PEG8000. At 8 dpi, intracellular HBV core antigen was stained with MAb 1C10 in green. Nuclei were stained with DAPI in blue (left). Secreted HBeAg in the supernatant was measured with commercial ELISA kit. A dotted line indicates the detection limit (right). (C) Human and mouse NTCP bound to pre-S1 lipopeptide. HepG2 cells were transfected as in panel A and were maintained in PMM for 24 h before staining with 400 nM FITC-labeled lipopeptide corresponding to the N-terminal 59

and HDV. We report that, although mNTCP is capable of binding to the pre-S1 lipopeptide and transporting taurocholate, it does not support HBV and HDV infection. This result is consistent with previous observation that mouse hepatocytes could bind to HBV pre-S1 but do not support viral infection (24–26). By making a series of human and mouse NTCP chimeras and point mutations, we show that the key determinant of mNTCP for viral infection locates in a small region of mNTCP containing aa 84 to 87. Remarkably, replacing aa 84 to 87 of mNTCP with human counterpart converted mNTCP into a fully functional receptor for HBV and HDV infection in HepG2 cells. Conversely, replacement of aa 84 to 87 of hNTCP with corresponding mouse residues led to a significant loss of hNTCP in supporting HBV and HDV infection. In addition, we demonstrated that aa 84 to 87 and aa 157 to 165 are both required to enable NTCP to accomplish pre-S1 lipopeptide binding and support the viral infections on HepG2 cells. Finally, we showed that various cell lines, regardless of their tissue or species origin, supported HDV infection when hNTCP or mNTCP with residues 84 to 87 replaced by human counterparts was provided. However, appreciable HBV infection in these cells was not detected under the conditions tested, underlining the different requirements of host factors between HBV and HDV. These studies elucidated molecular determinants of mNTCP for the restriction of viral entry of HBV and HDV and highlighted the central role of NTCP for HDV infection mediated by HBV envelope proteins.

MATERIALS AND METHODS

Cell lines. Human hepatocellular carcinoma cells (HepG2), Human cervical carcinoma cells (HeLa), African green monkey kidney epithelial cells (Vero), and Chinese hamster ovary cells (CHO) were from American Type Culture Collection (ATCC); human hepatocellular carcinoma cells (Huh-7) and mouse hepatocellular carcinoma cells (Hepa1-6) were from the Cell Bank of Type Culture Collection, Chinese Academy of Sciences. Mouse hepatocyte cell line MMHD3 was a gift from Erquan Zhang. These cells were cultured with Dulbecco modified Eagle medium (Invitrogen) supplemented with 10% fetal bovine serum (FBS), 100 U of penicillin/ml, and 100 μg of streptomycin/ml at 37°C in 5% CO_2 humidified incubator with regular passage every 2 to 3 days. After transfection of NTCP-expressing plasmids, the cells were cultured in PTH maintenance medium (PMM), which is Williams E medium supplemented with 5 μg of transferrin/ml, 10 ng of epidermal growth factor/ml, 3 μg of insulin/ml, 2 mM L-glutamine, 18 μg of hydrocortisone/ml, 40 ng of dexamethasone/ml, 5 ng of sodium selenite/ml, 2% dimethyl sulfoxide, 100 U of penicillin/ml, and 100 μg of streptomycin/ml. After viral inoculation, the cells were maintained in PMM alone or in PMM containing 2% FBS, with regular medium changing every 2 days.

Peptide, antibodies, and other reagents. myr-59-fluorescein isothiocyanate peptide (FITC-pre-S1), containing the first 59 residues of pre-S1 domain of HBV strain S472 (GenBank accession no. EU554535.1) with N-terminal myristoylation modification and C-terminal FITC conjugation, was synthesized by SunLight peptides, Inc. (Beijing, China). 1C10 is a mouse monoclonal antibody (MAb; subtype IgG1) against the HBV core protein; 4G5 is a mouse MAb (subtype IgG1) recognizing HDV delta antigen (11). Both MAbs were generated using conventional mouse hybridoma technology in the lab. 1D4 specifically recognizing C9 tag was purchased from Santa Cruz. C9 tag was derived from C-terminal 9 amino acids of rhodopsin with the amino acid sequence TETSQVAPA. Secondary antibodies for immunofluorescence staining or Western blot were from Life Technologies (USA) or Sigma-Aldrich (USA). Enzyme-linked immunosorbent assay (ELISA) kits for HBeAg detection were from Wantai Pharm, Inc. (Beijing, China). Quantitative real-time PCR kit and reverse transcriptase reagents were purchased from TaKaRa, Inc. (Beijing, China). Streptavidin-coupled magnetic beads (Dynabeads MyOne streptavidin T1) were purchased from Life Technologies. EZ-Link Sulfo-NHS-LC-Biotin was from Thermo Scientific (USA). [^{3}H]taurocholate with an activity of 5.0 Ci/mmol (0.185 TBq/mmol) and liquid scintillation cocktail (Ultima Gold XR) were purchased from Perkin-Elmer (USA). Other reagents were purchased from New England BioLabs (USA), Life Technologies (USA), or Sigma-Aldrich (USA).

Virus production. For HDV, a plasmid containing a head-to-tail trimer of 1.0× HDV cDNA of a genotype I virus under the control of a cytomegalovirus (CMV) promoter was used for the production of HDV RNPs. A pUC18 plasmid containing nucleotides 2431 to 1990 of HBV (genotype D, GenBank accession no. U95551.1) was used for expressing HBV envelope proteins under the control of endogenous HBV promoter. HDV viruses were produced by transfection of the plasmids in Huh-7 as previously described (11, 27). HBV was produced by transfection of Huh-7 with a plasmid containing 1.05 copies of HBV genome (genotype D, GenBank accession no. U95551.1) under the control of a CMV promoter as previously described (11, 28).

NTCP chimeras and mutants. Human and mouse NTCP were amplified using cDNA from primary human or mouse hepatocytes, respectively, and cloned into pcDNA6 vector with a C9 tag at the C terminus. NTCP chimeras were constructed using standard PCR-based fragment replacement. Human and mouse NTCP mutants were generated by mutagenesis using the QuikChange method (Stratagene). Sequences of all NTCP plasmids were confirmed by DNA sequencing.

[^{3}H]taurocholate uptake assay. [^{3}H]taurocholate uptake experiments were conducted according to a protocol previously described (29), with minor modifications. In brief, cells growing in a 48-well plate were preincubated for 10 min at 37°C in either Na^+ or choline$^+$ Ringer solution (Na^+ Ringer solution is composed of 145 mM NaCl, 4.8 mM KCl, 1.2 mM $MgSO_4$, 1.2 mM KH_2PO_4, 1.5 mM $CaCl_2$, 20 mM glucose, and 10 mM HEPES buffered with Tris [pH 7.4]; choline$^+$ Ringer solution is composed of 145 mM choline, 4.8 mM KCl, 1.2 mM $MgSO_4$, 1.2 mM KH_2PO_4, 1.5 mM $CaCl_2$, 20 mM glucose, and 10 mM HEPES buffered with Tris [pH 7.4]). Unless otherwise noted, the cells were then incubated with 1 μM [^{3}H]taurocholate for 15 min at 37°C in Na^+ Ringer solution. Cells were washed extensively with ice-cold phosphate-buffered saline (PBS) and then lysed by 100 μl of 1% Triton X-100 in water for 5 min, followed by mixing with 900 μl of liquid scintillation cocktail (Ultima

aa of pre-S1 (FITC-pre-S1) at 37°C for 3 h. Cells were washed extensively with culture medium to remove excess free peptide before visualization (left), or cells were detached by 5 mM EDTA-PBS, and the FITC-pre-S1 association was analyzed by flow cytometry (right). Shading indicates the pcDNA6 vector, the dotted line indicates mNTCP, and the solid line indicates hNTCP. Mean fluorescence of pre-S1 binding: vector, 13.66; mNTCP, 35.33; hNTCP, 67.99. (D) HepG2 cells were transfected as in panel A, and the total and cell surface NTCP expression were examined at 24 to 36 h posttransfection. For the total NTCP expression levels (upper panel), cell lysates were treated with PNGase F and separated by SDS-PAGE, followed by Western blotting with 1D4, which recognizes a C9 tag added to the C terminus of NTCP molecules. For the cell surface NTCP expression levels (middle panel), surface proteins were biotinylated and pulled down with streptavidin T1 Dynabeads. NTCP surface expression was then examined by Western blotting with MAb 1D4. The expression of GAPDH in the cell lysates is shown (bottom panel) as an internal control. (E) Uptake of [^{3}H]taurocholate ([^{3}H]TC) by HepG2 cells transfected with human NTCP, mouse NTCP, or vector pcDNA6. HepG2 cells were transfected and then cultured in PMM for 24 h. Cells were incubated at 37°C for 15 min with 1 μM [^{3}H]taurocholate diluted in Na^+ Ringer solution or choline$^+$ Ringer solution without Na^+. Intracellular accumulation of [^{3}H]taurocholate was determined by scintillation counting. The uptake efficiency is presented as counts per 100,000 HepG2 cells per min.

Gold XR) (Perkin-Elmer, USA). Liquid scintillation counting was performed on a Perkin-Elmer 1450 LSC liquid scintillation counter and luminescence counter.

FITC-pre-S1 peptide binding assay. Pre-S1 peptide binding assay was performed as previously described (11). In brief, cells transfected with plasmids expressing NTCP or variants were cultured in PMM. At 24 h after transfection, cells were incubated with 400 nM peptide containing the first 59 residues of pre-S1 domain with N-terminal myristoylation modification and C-terminal labeling of FITC (FITC-pre-S1) at 37°C for 3 h in the culture medium. After extensive washes with culture medium, the binding images were captured with a Nikon Eclipse Ti fluorescence microscope. For fluorescence-activated cell sorting (FACS) analysis, the FITC-pre-S1 stained cells without fixation were detached with 0.5 mM EDTA-PBS, washed, and resuspended in PBS with 0.5% bovine serum albumin (BSA) and analyzed with a FACS LSRII instrument (BD).

Viral infection on receptor-complemented cells. HepG2 or other cell lines were transfected with plasmids expressing NTCPs or their variants with Lipofectamine 2000 (Invitrogen) according to the manufacturer's instructions. Cells were cultured in PMM for 24 h after transfection and then inoculated with 100 multiplicities of genome equivalents (mge) of HBV or 500 mge of HDV at 37°C for 24 h in the presence of 5% polyethylene glycol (PEG). Medium was replenished every 2 days with PMM or PMM with 2% FBS.

Quantification of HDV RNA in cell samples. HDV-infected cells were lysed by TRIzol reagent, and the total RNA was isolated according to the manufacturer's instructions. The total RNA was reverse transcribed into cDNA with PrimeScript RT-PCR kit (TaKaRa), and 2 μl of cDNA was used for real-time PCR assay. The primers for quantifying HDV total RNA or genome equivalent copies are located in the delta antigen coding region of HDV RNA genome (forward primer HDV-1184F [5′-TCTTCC TCGGTCAACCTCTT-3′] and backward primer HDV-1307R [5′-ACAA GGAGAGGCAGGATCAC-3′]). Real-time PCR was performed on an ABI Fast 7500 real-time system instrument (Applied Biosystems, USA). The HDV viral genome equivalent copies were calculated with a standard curve and the cellular GAPDH (glyceraldehyde-3-phosphate dehydrogenase) RNA was used as an internal control.

Assays for HBV viral antigen HBeAg from supernatant of infected cells. Supernatants from infected cells expressing NTCP and their variants were collected at 3, 5, and 7 days postinfection (dpi). The secreted viral antigen HBeAg was examined using 50 μl of medium by ELISA with a commercial kit from Wantai Pharm, Inc. (Beijing, China), according to the manufacturer's instructions. All experiments were performed in duplicate and repeated at least two times independently.

Immunofluorescence microscopy analysis of intracellular antigens. For HDV infection, cells transfected with NTCP-expressing or control plasmid were infected with HDV at 37°C for 24 h in the presence of 5% PEG. At 8 dpi, the cells were treated with 100% methanol at room temperature for 10 min and then stained with 10 μg of FITC-conjugated mouse anti-delta antigen MAb, 4G5/ml, as previously described (11). Images were captured with an Eclipse Ti fluorescence microscope (Nikon) and a representative picture is shown. To quantify the infection ratio, ~6,000 cells were analyzed by the Columbus Image Data Storage and Analysis System (Perkin-Elmer). To record HBV infection, infected cells were washed with cold PBS for three times and fixed in 3.7% paraformaldehyde at room temperature for 10 min. The cells were then permeabilized with 0.5% Triton X-100 for 10 min at room temperature and blocked with 3% BSA at 37°C for 1 h, followed by incubation with 5 μg of mouse MAb 1C10/ml, which recognizes HBcAg, and then FITC-conjugated secondary antibody. In addition, 2 μg of DAPI (4′,6′-diamidino-2-phenylindole)/ml was also added to stain the cell nucleus. The stained cells were imaged with a Nikon Eclipse Ti fluorescence microscope.

Analysis of the total and surface protein expression of human NTCP (hNTCP), mouse NTCP (mNTCP), or NTCP variants. HepG2 or Hepa1-6 cells transfected with human or mouse NTCPs or their variants were cultured in PMM for 24 h after transfection. For examination of cell surface expression, the transfected cells were surface biotinylated with sulfo-NHS-LC-biotin (Pierce) according to the manufacturer's instructions. The biotinylated cells were then lysed in 600 μl of 1× radioimmunoprecipitation assay (RIPA, pH 7.4) buffer containing 20 mM Tris, 150 mM NaCl, 0.1% sodium dodecyl sulfate (SDS), 0.5% sodium deoxycholate, 1% NP-40, and 1× protease inhibitor cocktail (Roche). Protein concentration in the lysate was determined by Bio-Rad DC protein assay. Surface-biotinylated NTCP proteins in the cell lysate of ~160 μg of total cellular protein were pulled down by ~300 μg of streptavidin T1 Dynabeads. After extensive washing with 1× radioimmunoprecipitation assay (RIPA) buffer, bound NTCP proteins were eluted by boiling for 5 min in 1× SDS-PAGE protein sample buffer, followed by treatment with PNGase F (NEB) according to the manufacturer's instructions. The treated sample were separated by SDS-PAGE and subsequently detected by Western blotting with anti-C9 MAb (1D4) that recognizes the C9 tag fused at the C terminus of NTCPs. To compare NTCP total expression level, wild-type or mutant NTCP plasmids transfected cells were lysed with 1× RIPA buffer and treated with PNGase F at 24 h posttransfection. The treated cell lysates, each containing ~8 μg of total cellular protein were subjected to SDS-PAGE without boiling, followed by Western blotting with 1D4. The expression level of GAPDH was used as an internal control.

RESULTS

mNTCP does not support HBV and HDV infection but is capable of pre-S1 binding. In order to elucidate the molecular mechanism of the host restriction of HBV and HDV infection in mice, mNTCP was cloned and exogenously expressed in HepG2 cells for testing its activity in supporting viral infection and the pre-S1 peptide binding. As shown in Fig. 1A and B, mNTCP failed to render HepG2 susceptible for HDV or HBV infection, a finding consistent with the host restriction in mouse. Consistent with the observations that the pre-S1 lipopeptide can bind to mouse hepatocytes (25, 26, 30), mNTCP bound to preS1-FITC peptide, although at a lower efficiency than that of hNTCP (Fig. 1C), a finding that cannot be explained by protein expression level or distribution since these were expressed at a similar level on the cell surface (Fig. 1D). In addition, mNTCP can mediate taurocholate uptake in the presence of sodium as efficient as hNTCP (Fig. 1E).

We have previously shown that aa 157 to 165 of hNTCP is critical for pre-S1 binding and viral infection; mkNTCP neither supported pre-S1 peptide binding nor viral infection in HepG2 cells unless the 157 to 165 residues were replaced by the human counterpart (11). However, mNTCP is very similar to hNTCP in this small region, indicating that aa 157 to 165 is probably not the restriction determinant in mNTCP. Sequence alignment of NTCPs showed that mNTCP markedly differs from hNTCP at the C terminus (Fig. 2A). However, exchanging the C-terminal aa 300 to 349 of hNTCP and aa 300 to 362 of mNTCP did not alter their activities in supporting pre-S1 binding or HDV infection (Fig. 2B), suggesting that determinants other than aa 157 to 165 and the C terminus of NTCP may also contribute to the efficiency of viral infection.

HBV and HDV viral entry is primarily restricted by a region of mNTCP containing 95 residues. The major isoform of mNTCP contains 362 amino acids and shares 73.8% sequence similarity with hNTCP, the different residues scattered across the entire molecule. We first attempted to identify the key region that limits viral entry of HBV and HDV. A set of domain-swapped chimeras of hNTCP and mNTCP were constructed. Based on sequence alignment and topology prediction (Fig. 2A) (31), NTCP could be divided into five domains from A to E. For loss of function assay, swapping chimeras were generated by replacing each domain of hNTCP with the mouse counterpart, separately (Fig. 3A). For gain-of-function assay, regions of mNTCP were

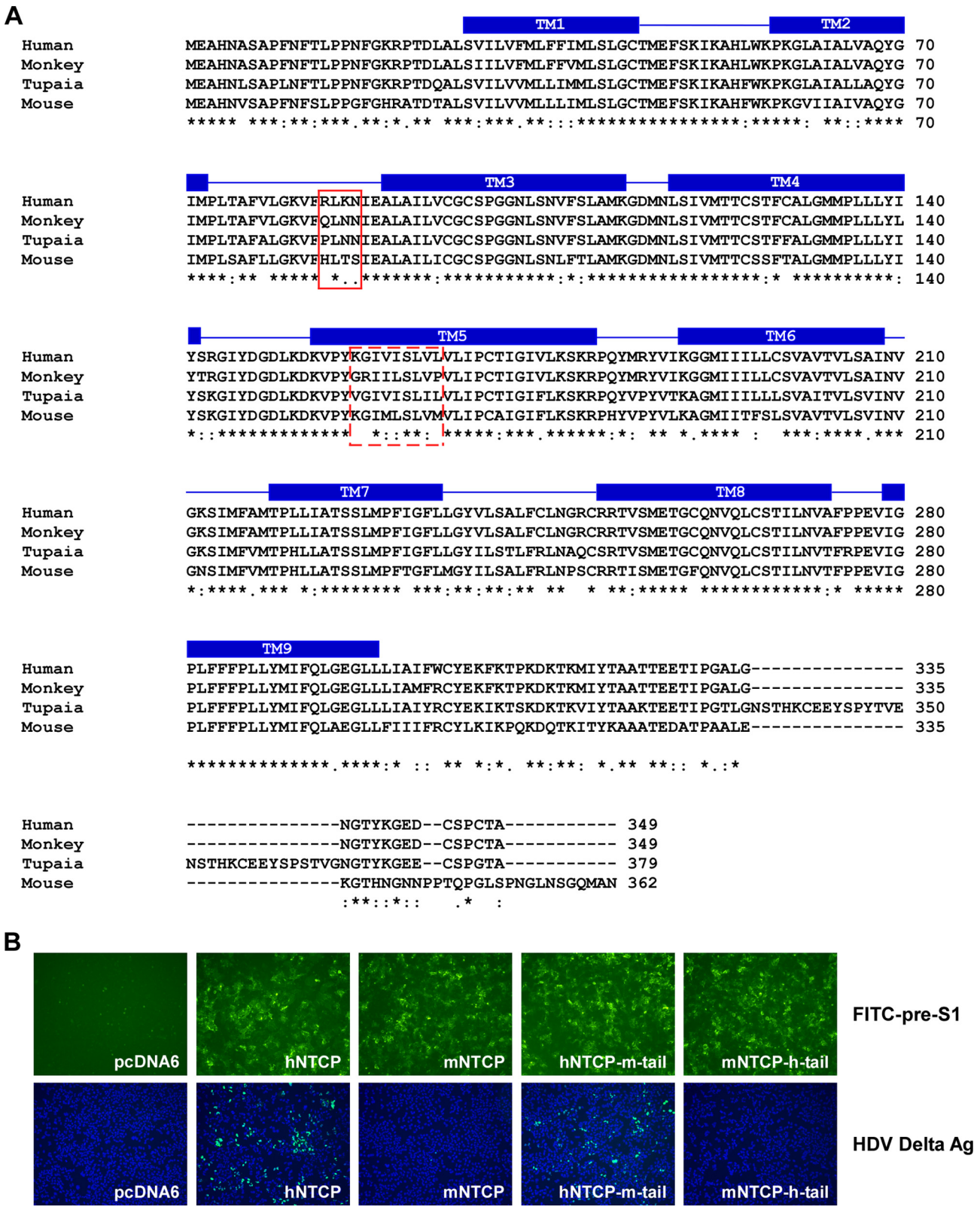

FIG 2 Exchange of the cytosolic tails of mouse and human NTCPs did not alter their abilities to support HDV infection. (A) NTCPs from human, crab-eating monkey, tupaia, or mouse (GenBank accession nos. NM003049, XM001110268, JQ608471, and NM001177561) were aligned using ClustalW2. Blue bars indicate transmembrane domains that were predicted by alignment of human NTCP with NTCPs from other species and were based on the crystal structure of a bacterial homologue of the bile acid sodium symporter $ASBT_{NM}$ with small modifications. The boxed residues (aa 84 to 87, solid line; aa 157 to 165, dotted line) indicate motifs that are crucial for FITC-pre-S1 binding and viral infections. (B) Human NTCP, mouse NTCP, pcDNA6 vector, hNTCP with aa 300 to 362 cytosolic tail of mNTCP (hNTCP-m-tail), or mNTCP with aa 300 to 349 cytosolic tail of hNTCP (mNTCP-h-tail) were transfected in Huh-7 cells and cultured in PMM for 24 h. The cells were incubated with 400 nM FITC-pre-S1 peptide at 37°C for 3 h and then imaged after extensive washing (upper panels), or the cells were inoculated with 500 mge of HDV at 37°C for 24 h in the presence of 5% PEG8000, the HDV delta antigen in infected cells was detected with FITC-conjugated MAb 4G5 at 8 dpi, and the cell nuclei were counterstained with DAPI (blue, lower panels).

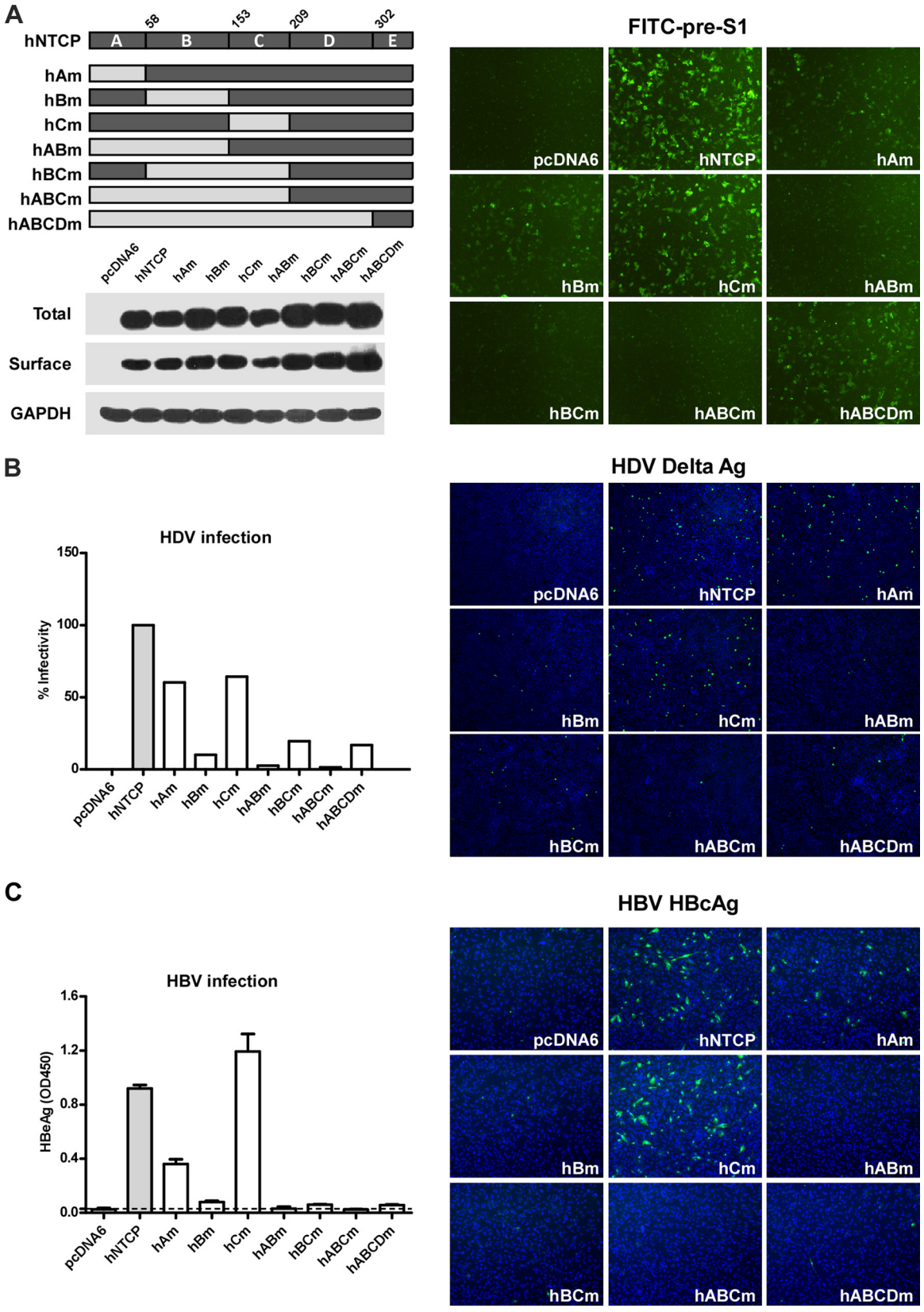

FIG 3 HBV and HDV entry is primarily restricted by a region of mNTCP containing 95 residues. (A) Schematic diagram of chimeric NTCP proteins (upper panel, left). hNTCP (dark gray) and mNTCP (light gray) were divided into five parts (A to E) based on sequence alignment and topology prediction (30). Swap chimeras of hNTCP and mNTCP were generated by stepwise exchange of these domains for loss-of-function and gain-of-function assays. Western blot analysis of the total and surface expression levels of different NTCP chimeras in transfected HepG2 cells was performed. GAPDH protein was used as an internal control

stepwise replaced by corresponding human residues (Fig. 4A). All of these chimeras were cloned into pcDNA6 vector with a C-terminal tag (C9). The total and surface expression levels of all of the wild-type and chimeric mutant NTCPs were examined. As shown in Fig. 3A and 4A, all NTCPs were well expressed and can be efficiently sorted to the surface of HepG2 cells. NTCPs with mouse backbone frequently showed slightly higher expression levels than those with human backbone. However, various NTCP chimeras bound to FITC-pre-S1 peptide with different efficiency, underlining determinants important for the binding. In addition, all NTCP chimeras were able to uptake ^{3}H-labeled taurocholate at an efficiency similar to that of the wild-type NTCPs, indicating that the overall structural integrity of the proteins for all chimeras was not impaired (data now shown). These chimeras were then examined for supporting viral infections. As shown in Fig. 3B and C and Fig. 4B and C, domain B (aa 58 to 152), 95 aa in length, was crucial for HDV and HBV infection. All of the swapping mutants containing domain B of mNTCP, including hBm, hABm, hBCm, hABCm, and hABCDm, markedly lost their abilities in supporting viral infection on HepG2 cells. On the other hand, in gain-of-function assays, viral infections can be restored in HepG2 cells transfected with chimeras containing the domain B of hNTCP (mBh, mABh, mBCh, mABCh, or mABCDh). Taken together, these results suggested that the region of aa 58 to 152 of mNTCP was responsible for the inability of mNTCP in supporting HBV and HDV viral entry.

Residues 84 to 87 of mNTCP compose a key motif limiting viral infection. In the region of aa 58 to 152, there are 12 differing residues between mNTCP and hNTCP. We therefore made a series of hNTCP variants in which one or a few residues were altered to their mouse counterparts (hNTCP-T75S, hNTCP-m84-87, hNTCP-S109T, hNTCP-T127S, and hNTCP-C129T) and the corresponding mNTCP variants with human counterparts (mNTCP-S75T, mNTCP-h84-87, mNTCP-T109S, mNTCP-S127T, and mNTCP-T129C). All of these NTCPs expressed at similar levels for both total and surface expression (Fig. 5A and 6A). The transporting efficiency of these NTCPs, indicated by [^{3}H]taurocholate uptake in HepG2 cells transfected with the variants, was also comparable to that of wild-type NTCPs (data not shown). Remarkably, the introduction of mouse residues 84 to 87 (His-Leu-Thr-Ser), which presumably are located at the first extracellular loop of NTCP, into hNTCP dramatically inhibited HBV and HDV infection, whereas other residues tested had no significant effect on the infection; conversely, replacing mNTCP residues 84 to 87, but not other residues, with the corresponding human residues (Arg-Leu-Lys-Asn) resulted in enhanced FITC-pre-S1peptide binding and effectively converted mNTCP into a functional receptor for HBV and HDV infection (Fig. 5B and C and Fig. 6B and C). The three different residues within aa 84 to 87 between mNTCP and hNTCP contributed to infection restriction at different levels, with residue 87 being the most significant one (Fig. 7D and E), while the efficiency of [^{3}H]taurocholate uptake and the protein expression levels of all of them were similar (Fig. 7A and B). These residues were also tested for their contributions in the binding of NTCP with pre-S1. Consistent with the infection data, the alteration of aa 84 to 87 in hNTCP reduced the binding activity of hNTCP with pre-S1 peptide, whereas substitution of the corresponding residues of mNTCP with human counterparts increased its pre-S1 binding activity (Fig. 7C).

Amino acids 84 to 87 and aa 157 to 165 of NTCP are required for HBV and HDV infection. We have previously reported that residues 157 to 165, the most divergent region between hNTCP and mkNTCP, critically contributed to pre-S1 binding and to viral infection on the receptor-complemented HepG2 cells. In the present study, we revealed that alteration of another critical motif, aa 84 to 87, could convert mNTCP to a functional receptor for HBV and HDV infection. To further investigate the functionality of these two regions in pre-S1 binding and viral entry, we introduced monkey aa 157 to 165 into the corresponding sites in mNTCP and mNTCP mutant containing human residues of 84 to 87 (mNTCP-h84-87). All of these NTCP mutants were expressed at similar level (Fig. 8A, left). Both mNTCP and mNTCP-h84-87 were capable of binding to pre-S1 peptide, while only mNTCP-h84-87 supported viral infection. Substitution of aa 157 to 165 with residues from mkNTCP on wild-type mNTCP or mNTCP-h84-87 led to a complete loss of pre-S1 binding activity (Fig. 8A, right). As expected, the substitution also abolished viral infection on mNTCP-h84-87 (Fig. 8B and C). These results suggested that both regions, aa 84 to 87 and aa 157 to 165, were critically important for viral entry and substantially contributed to HBV and HDV infection.

NTCP confers cells from different tissue and species susceptibility for HDV infection. In order to examine whether viral infection of HBV and HDV in mouse is only limited by mNTCP, we tested hNTCP, mNTCP, hNTCP bearing aa 84 to 87 from mNTCP, and mNTCP variants with residue substitutions for their ability in supporting viral entry in a mouse hepatoma cell line Hepa1-6 and other cell lines. The [^{3}H]taurocholate uptake efficiency (Fig. 9A) and the total and surface expression of all NTCPs were comparable among all variants tested in Hepa1-6 cells (Fig. 9B). Consistent with results obtained from HepG2 cells, Hepa1-6 cells transfected with hNTCP, mNTCP-h84-87, and to a lower extent mNTCP, but not hNTCP-m84-87 bound to the pre-S1 peptide, whereas only hNTCP and mNTCP-h84-87 support HDV infection (Fig. 9C, top panel). We also verified the contribution of individual residues 84, 86, and 87 on HDV infection in Hepa1-6 cells, with results similar to that from HepG2 cells (data not shown). These results suggested that mNTCP was a major if not the only restriction factor for HDV infection in mouse cells.

In addition to Hepa1-6 cells, several other cells from different tissues and species, including MMHD3 (mouse hepatocarci-

(lower panel, left). The cells were incubated with 400 nM FITC-pre-S1 peptide at 37°C for 3 to 4 h, and images were captured with a Nikon Eclipse Ti fluorescence microscope after extensive washes with culture medium (right). (B) HDV infection mediated by NTCP chimeras. HepG2 cells transfected with NTCP chimeras were infected with 500 mge of HDV particles in the presence of 5% PEG8000. At 8 dpi, HDV delta antigen was stained with FITC-conjugated MAb 4G5 (right). Images were analyzed by Columbus Image Data Storage and Analysis System, and the ratio of infected cells was calculated as the ratio of delta antigen-positive dots to the number of nuclei. Infectivity was presented as percentage of HDV infection on wild-type hNTCP (left). (C) HBV infection mediated by NTCP chimeras. HepG2 cells were transfected as in panel B and inoculated with 100 mge of HBV particles in the presence of 5% PEG8000. Secreted HBeAg in the supernatant was measured at 6 dpi with a commercial ELISA kit; the dotted line indicates the detection limit (left). At 7 dpi, the cells were stained with 5 μg of HBcAg-specific MAb 1C10/ml. Cell nuclei were stained with DAPI in blue. Representative pictures of the infections were shown (right).

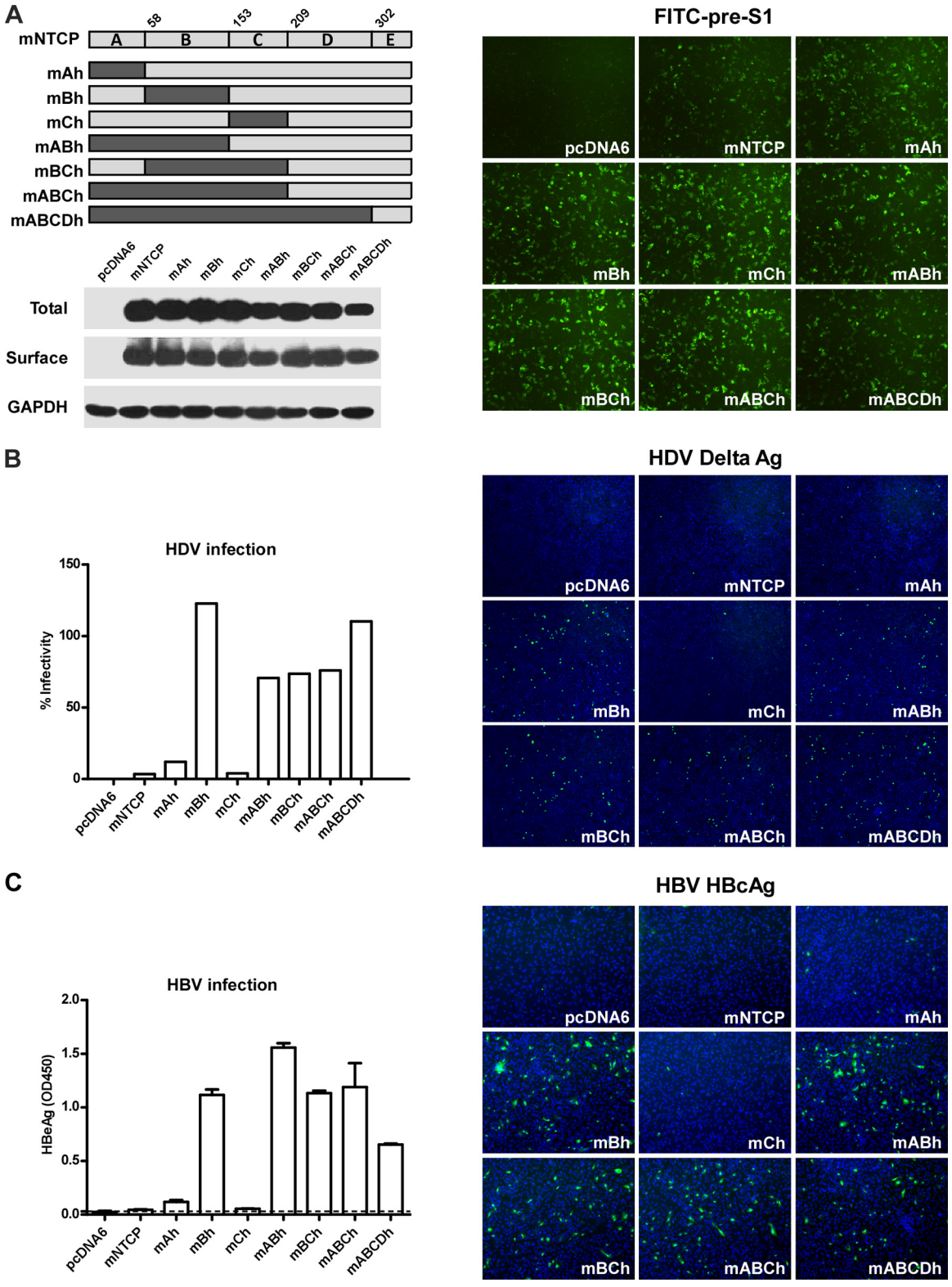

FIG 4 Substitution of the 95 residues fragment of mNTCP with hNTCP counterpart converts mNTCP a functional receptor on HepG2 cells. (A) Schematic diagram of chimeric NTCP proteins (upper panel, left): hNTCP (dark gray) and mNTCP (light gray). Western blot analysis of the total and surface expression levels of different NTCP chimeras in transfected HepG2 cells was performed. GAPDH protein was used as an internal control (lower panel, left). Cells were incubated with 400 nM FITC-pre-S1 peptide at 37°C for 3 to 4 h, and images were captured after extensive washes with culture medium (right). (B) HDV infection mediated by NTCP chimeras. HepG2 cells transfected with NTCP chimeras were infected with 500 mge of HDV particles in the presence of 5% PEG8000. At 8 dpi, the HDV delta antigen was stained with MAb 4G5 in green (right). The ratio of infected cells were evaluated as the ratio of delta antigen-positive dots to the number of nuclei. Infectivity is presented as the percentage of HDV infection on wild-type hNTCP (left). (C) HBV infection mediated by NTCP chimeras. HepG2 cells were transfected as in panel B and were inoculated with 100 mge of HBV particles in the presence of 5% PEG8000. Secreted HBeAg in the supernatant was measured at 6 dpi, and the dotted line indicates the detection limit (left). At 7 dpi, the cells were stained with 1C10 in green. Representative pictures of the infections are shown (right).

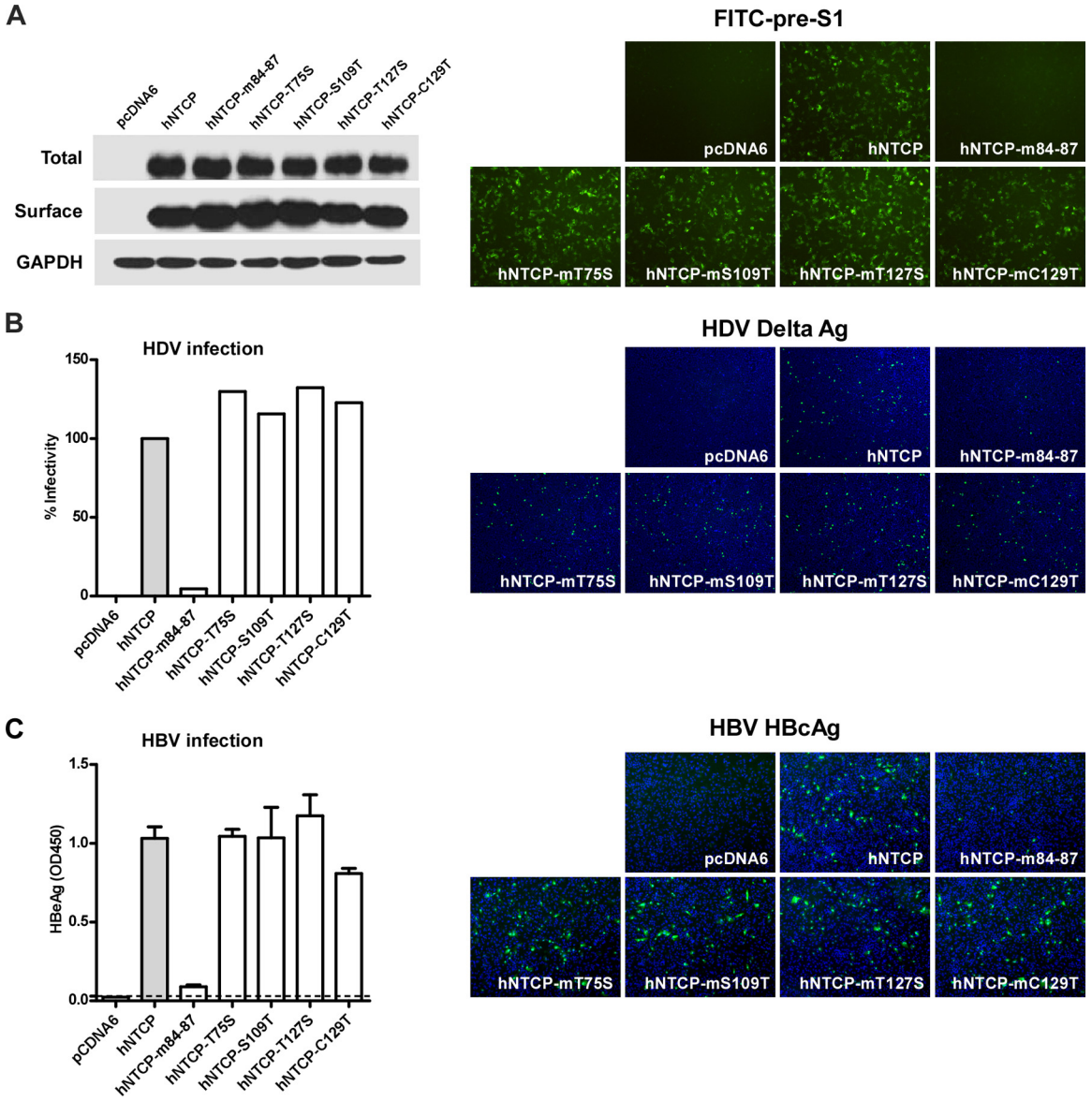

FIG 5 Residues 84 to 87 of mNTCP compose a key motif limiting viral infection. (A) Western blot analysis of the total and surface expression levels of NTCP in HepG2 cells transfected with NTCP variants. The GAPDH level in the cell lysates was used as an internal control (left). Cells were incubated with 400 nM FITC-pre-S1 peptide at 37°C for 3 to 4 h, and images were captured with a Nikon Eclipse Ti fluorescence microscope after extensive washes with culture medium (right). (B) HDV infection mediated by NTCP variants. HepG2 cells transfected as in panel A were infected with 500 mge of HDV, and the delta antigen was stained with FITC-labeled 4G5 at 8 dpi (right). Images were analyzed by Columbus software, and the ratio of infected cells were evaluated as the ratio of delta antigen-positive dots to the number of nuclei. Infectivity is presented as the percentage of HDV infection on wild-type hNTCP (left). (C) HBV infection mediated by NTCP variants. HepG2 cells transfected as in panel A were inoculated with 100 mge of HBV in the presence of 5% PEG8000. Secreted HBeAg in the supernatant was measured at 6 dpi with ELISA, and a dotted line indicates the detection limit (left). At 7 dpi, HBcAg was stained with MAb 1C10 in green. Cell nuclei were stained with DAPI in blue. Representative pictures of the infections are shown (right).

noma), HeLa (human cervical cancer), CHO (Chinese hamster ovary), and Vero (African green monkey kidney) cells were also examined (Fig. 9C). Strikingly, HDV infected all of these cells complemented with hNTCP or mNTCP-h84-87, similar to that of HepG2 cells. These data further demonstrated that host range as well as liver tropism of HDV infection might be predominantly determined at the receptor level. However, inoculations of hNTCP complemented Hepa1-6 or MMHD3 cells with HBV did not lead to appreciable viral infection (data not shown), indicating that HBV, unlike HDV, requires additional host factors for infection or that other host factor(s) may differentially regulate the life cycles of HBV and HDV.

DISCUSSION

Hepadnaviruses show remarkable species specificities, and their infection in species other than the natural hosts is usually limited by entry and postentry restrictions. NTCP is a cellular receptor for HBV and HDV and functions at the entry level. Crab-eating monkey NTCP neither bound to HBV pre-S1 peptide nor supported viral infection of HBV and HDV, but alter-

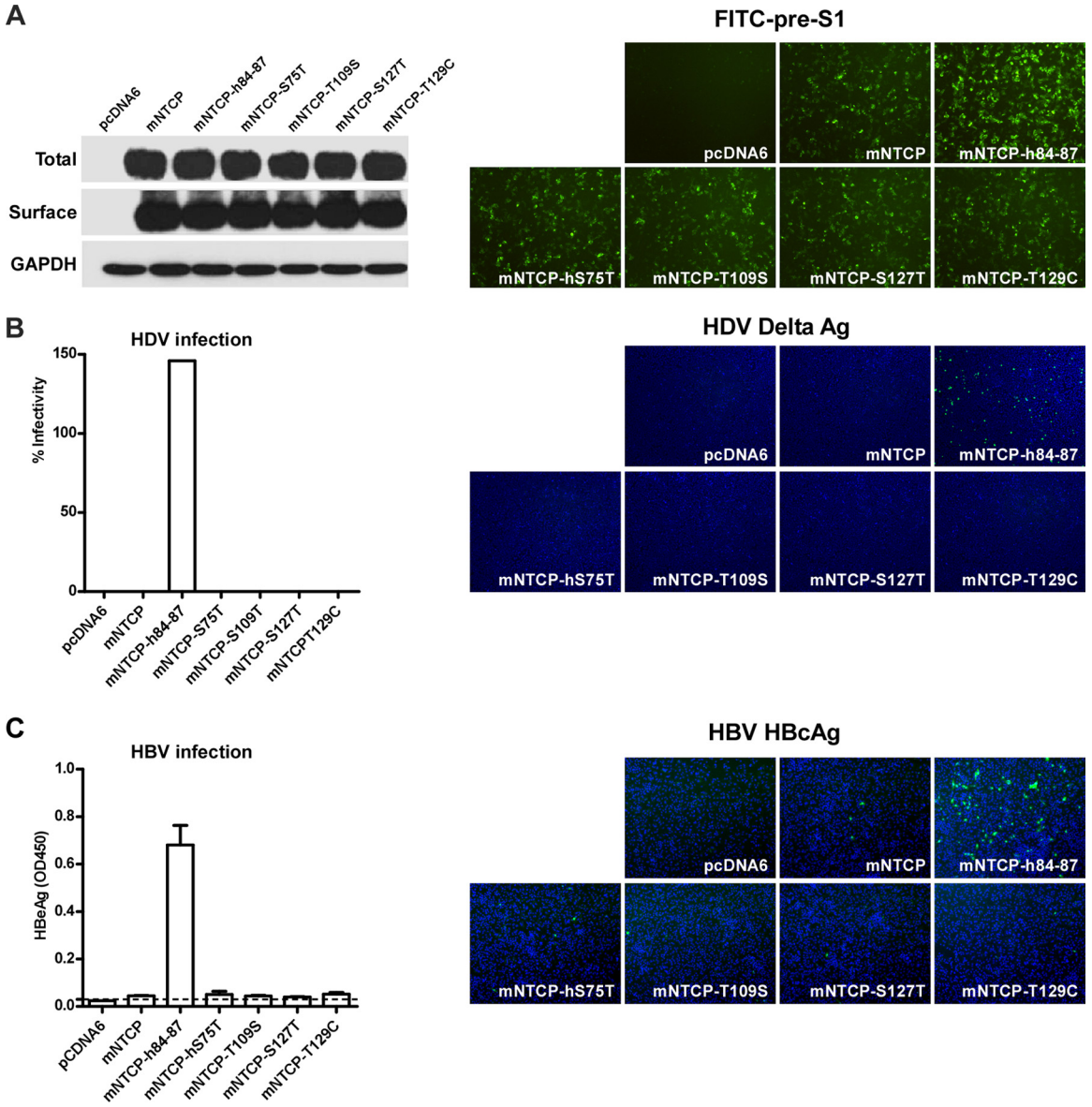

FIG 6 mNTCP bearing residues 84 to 87 from hNTCP supports viral entry on HepG2 cells. (A) Western blot analysis of the total and surface expression levels of NTCP in HepG2 cells transfected with NTCP variants. The GAPDH level in the cell lysates was used as an internal control (left). The cells were incubated with 400 nM FITC-pre-S1 peptide at 37°C for 3 to 4 h before images were recorded (right). (B) HDV infection mediated by NTCP variants. HepG2 cells transfected with the indicated NTCP variants were infected with 500 mge of HDV, and the delta antigen was stained with 4G5 in green at 8 dpi (right). Images were analyzed by Columbus software, and the ratio of infected cells was calculated as the ratio of delta antigen-positive dots to the number of nuclei. Infectivity is presented as the percentage of HDV infection on wild-type hNTCP (left). (C) HBV infection mediated by NTCP variants. HepG2 cells transfected as in panel B were inoculated with 100 mge of HBV in the presence of 5% PEG8000. Secreted HBeAg was measured at 6 dpi with ELISA, and the dotted line indicates the detection limit (left). At 7 dpi, cells were stained with 1C10 for HBcAg in green. Cell nuclei were in blue. Representative pictures of the infections were shown (right).

ation of only a small motif of aa 157 to 165 to human counterpart converted mkNTCP to a functional receptor for both pre-S1 binding and viral infections (11).

In the present study, we investigated molecular determinants that restrict mouse NTCP for viral entry of HBV and HDV. We first examined the region of aa 157 to 165 in mNTCP protein sequence and found only insignificant difference from human NTCP in this region. The inability of HBV and HDV to infect mouse is therefore unlikely determined by this motif of mNTCP, rather by other regions of NTCP, or yet-unknown limiting cellular factor(s) at entry, or postentry steps, or both. Because the difference between mNTCP and hNTCP protein sequences are scattered across the entire molecule, we constructed a comprehensive series of NTCP variants by swapping large fragment between mouse and human NTCP and followed by introducing point mutations to defined regions. We extensively examined pre-S1 lipopeptide binding and viral infections mediated by these variants. To rule out the possibility that observed binding or viral infection difference was due to abnormal protein expression or surface sorting efficiency of NTCPs, both the total and the surface expression levels of all the NTCP variants were verified. In addition, we also evaluated the transporting activity of NTCP variants for tauro-

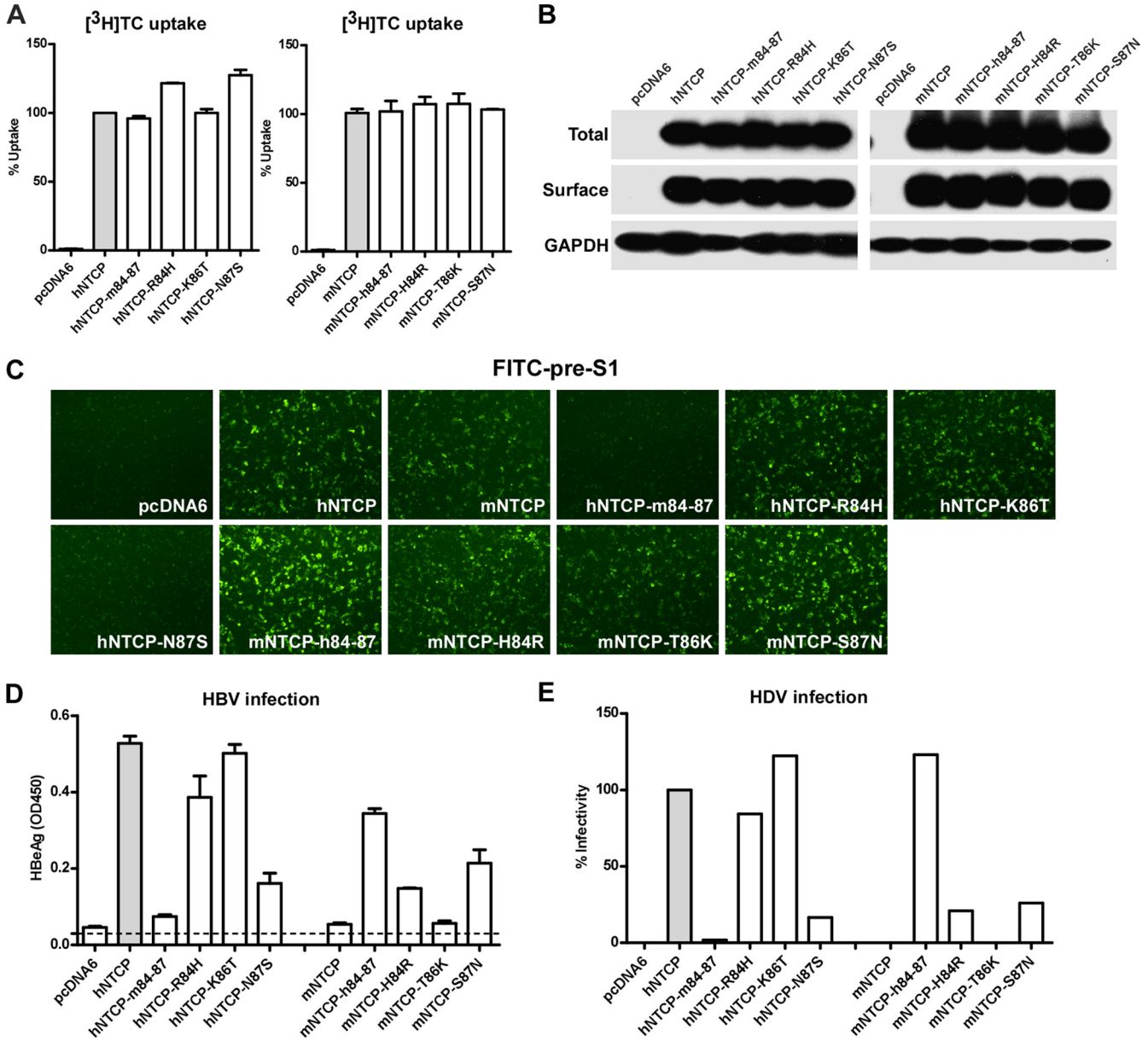

FIG 7 Contributions of the individual residues within aa 84 to 87 motif for NTCP as a viral receptor. (A) HepG2 cells transfected with NTCP variant bearing one or a few mutations within the aa 84 to 87 motif were cultured in PMM for 24 h. The uptake of [^{3}H]taurocholate ([^{3}H]TC) was quantified by scintillation counting and is presented as the percentage of that of hNTCP for hNTCP variants or as a percentage of that of mNTCP for mNTCP variants. (B) HepG2 cells were transfected as in panel A, and the total and surface expression levels of the NTCPs were examined by Western blotting. The level of GAPDH was used as an internal control. The data are presented as relative scintillation counts compared to hNTCP (left) or mNTCP (right). (C) HepG2 cells were transfected as in panel A and then stained with 400 nM FITC-pre-S1 at 37°C for 3 h before image recording. (D and E) HepG2 cells transfected as in panel A and then inoculated with 500 mge of HDV or 100 mge of HBV. (D) Secreted HBeAg in the supernatant were determined at 7 dpi with ELISA. (E) At 8 dpi, intracellular delta antigens were analyzed by staining with FITC-conjugated 4G5, quantified by Columbus software, and was presented as a percentage of infectivity of HDV on hNTCP.

cholate to ensure that the overall protein integrity of these variants was not impaired. Through the initial swapping mutant studies, a region of 95 residues (aa 58 to 152) of mNTCP was found to be responsible for limiting the receptor in supporting HBV and HDV entry. Further mapping studies identified residues aa 84 to 87 of mNTCP, which presumably are located at the first extracellular loop (Fig. 2), as the critical determinant restricting viral entry of HBV and HDV via this receptor. Consistently, the substitution of aa 84 to 87 (Arg-Leu-Lys-Asn) of hNTCP with the mouse counterpart (His-Leu-Thr-Ser), in particular, mutation N87S, significantly decreased pre-S1 binding and viral infection. Not surprisingly, substitution of aa 157 to 165 with residues from monkey NTCP led to significant loss of pre-S1 binding on both wild-type mNTCP and mNTCP-h84-87. These results indicated that receptor recognition by the pre-S1 is mediated or modulated at least by two regions of NTCP, one containing aa 84 to 87 and the other one with aa 157 to 165. However, it is difficult to predict the exact binding mode of pre-S1 lipopeptide with NTCP without struc-

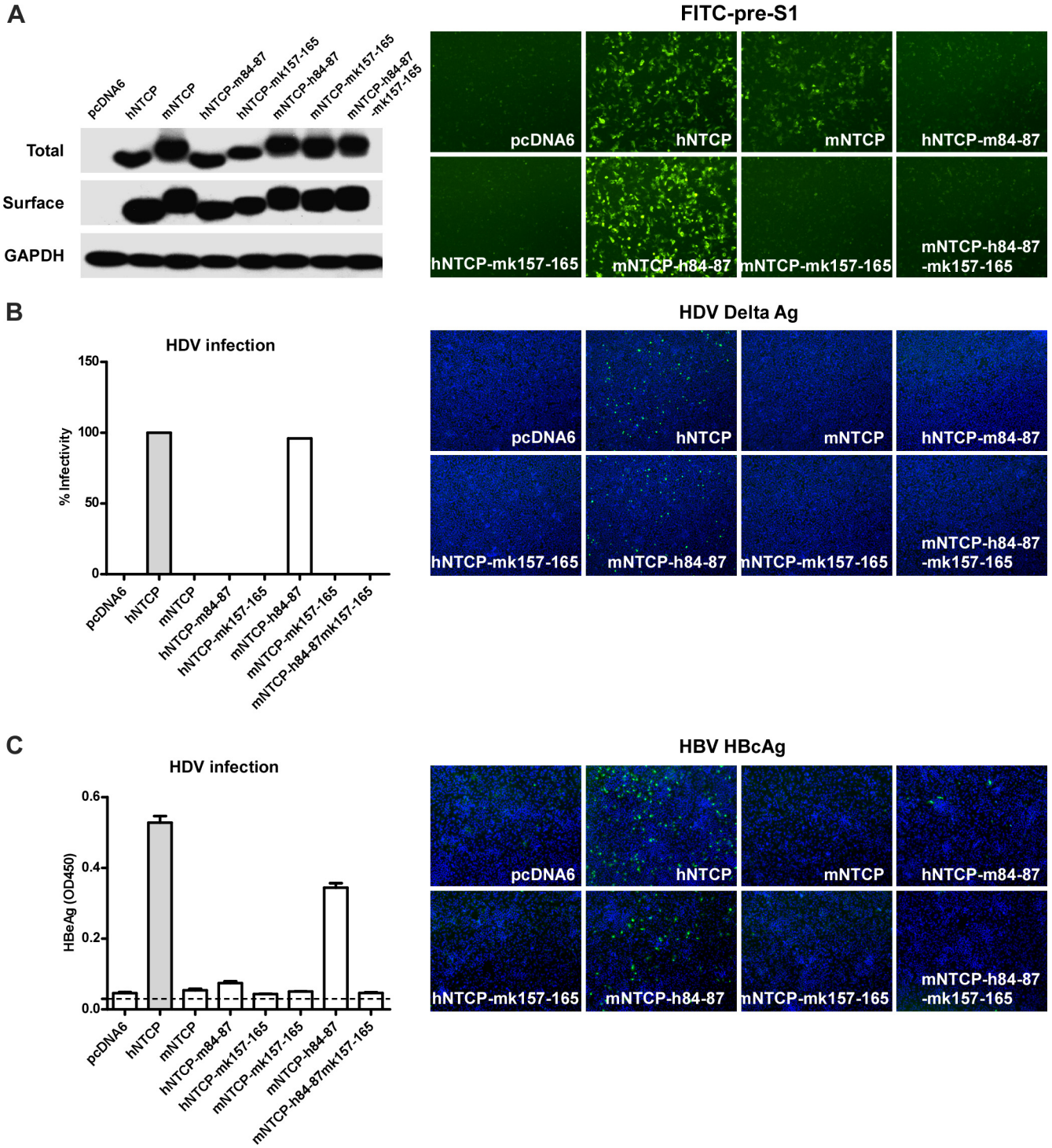

FIG 8 Amino acids 84 to 87 and aa 157 to 165 of NTCP are both required for HBV and HDV infection. (A) HepG2 cells were transfected with human NTCP, mouse NTCP, a pcDNA6 vector control, or NTCP variants as indicated and maintained in PMM for 24 h. The total and surface expression levels of different NTCP variants in transfected HepG2 cells were determined by Western blotting. GAPDH was used as an internal control (left). Other cells were stained with 400 nM FITC-pre-S1 peptide at 37°C for 3 h, followed by extensive washings, and then recorded (right). (B and C) HepG2 cells were transfected as in panel A and cultured in PMM for 24 h, followed by inoculation with 500 mge of HDV or 100 mge of HBV. (B) At 8 dpi, HDV infection, as indicated by intracellular delta antigens staining with FITC-conjugated 4G5 (right), was quantified by Columbus software and is presented as a percentage of the infectivity of HDV on hNTCP (left). (C) Secreted HBeAg in the supernatants was determined with ELISA (left), and intracellular core antigen was stained by 1C10 at 7 dpi (right).

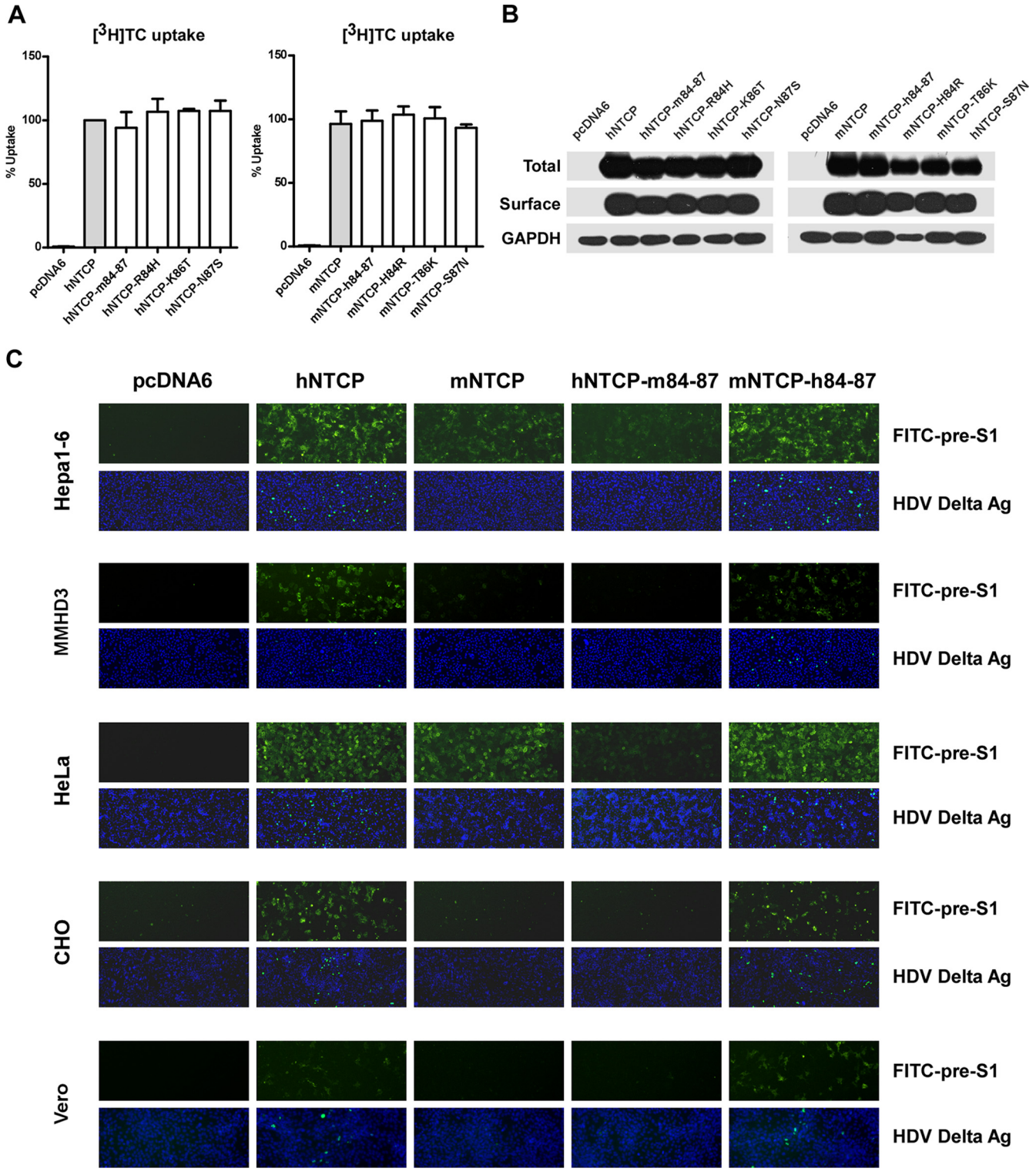

FIG 9 NTCP confers cells from different tissue and species susceptibility for HDV infection. (A) Mouse hepatocellular carcinoma cells (Hepa1-6) were transfected with human NTCP, mouse NTCP, pcDNA6 vector, or mutant NTCPs as indicated and cultured in PMM for 24 h, followed by incubation with 1 μM [^{3}H]taurocholate ([^{3}H]TC) in Na^+ Ringer solution at 37°C for 15 min. The uptake of [^{3}H]taurocholate was determined by scintillation counting and is presented as a percentage of that of hNTCP (left) or mNTCP (right). (B) Hepa1-6 cells were transfected as in panel A, and then the total and surface expression levels of NTCPs were examined by Western blotting. GAPDH was used as an internal control. (C) Hepa1-6 cells, mouse hepatocarcinoma cells (MMHD3), human cervical carcinoma cells (HeLa), Chinese hamster ovary cells (CHO), and African green monkey kidney cells (Vero) were transfected with human NTCP, mouse NTCP, human NTCP variant hNTCP-m84-87, mouse NTCP variant mNTCP-h84-87, or pcDNA6 vector as indicated and cultured in PMM for 24 h. The cells were stained with FITC-pre-S1 peptide or infected with 500 mge of HDV. For peptide staining, the cells were incubated with 400 nM FITC-pre-S1 peptide at 37°C for 3 h and then imaged after extensive wash (upper panel in each group). HDV delta antigen in infected cells was detected with FITC-conjugated MAb 4G5 at 8 dpi (lower panel in each group).

tural information of the pre-S1-NTCP complex. Comparing to aa 157 to 165 region that contains multiple hydrophobic residues, aa 84 to 87 are more likely exposed to extracellular solvents directly or constantly, indicating that they may directly involve in the binding. On the other hand, aa 157 to 165 may be critical for maintaining a conformation of NTCP important for pre-S1 binding and thereby affecting binding or can only be exposed after a conformational change triggered by a very early entry event. Taken together, we speculate that after virion attachment to hepatocytes via liver heparan sulfate proteoglycan (HSPG) (32, 33) or other, yet-unknown molecule(s), a high-affinity virus binding mediated by NTCP may be initiated by the interaction between aa 84 to 87 of NTCP with a region of pre-S1 (aa 2 to 47) (not necessarily the receptor binding motif [aa 9 to 15]), followed by further exposure of an increased number of binding sites on NTCP, and subsequently trigger a zipper-mode binding cascade between NTCP and the receptor binding sites and/or other involved regions of pre-S1 on the virion.

We showed that mNTCP could bind to pre-S1 peptide, albeit at a lower efficiency comparing to hNTCP. This result is in agreement with several recent reports showing that a similar pre-S1 lipopeptide competently bound to mouse hepatocytes *in vitro* and *in vivo* (24–26). Meier et al. showed that myristoylated pre-S1 domain mediated specific binding to differentiated but not dedifferentiated mouse hepatocytes *in vitro* (25). An early report also indicated that the pre-S1 lipopeptide not only bound to tree shrew hepatocytes transplanted into immunodeficient mice but also bound to mouse liver cells (26). This discrepancy between binding and mediating viral entry is not limited to mouse NTCP; the pre-S1 lipopeptide was also found binding in livers of rat and dog *in vivo* (30). In the present study, by studying the interaction between the pre-S1 lipopeptide (first 59 residues of pre-S1 domain of HBV L protein, genotype C) and the mNTCP variants, we found that binding of the pre-S1 domain to mNTCP is necessary but insufficient for supporting viral infection on target cells. It is intriguing how mNTCP, with a taurocholate transporting activity apparently similar to that of hNTCP and with considerable ability to bind to the lipopeptide and HDV virions, is still not sufficient to achieve HDV entry. This may be partially explained by the relative weaker binding affinity of mNTCP to pre-S1 and virions compared to hNTCP or because the binding is inefficient to trigger molecular events important for viral endocytosis and entry, or other unknown mechanisms, which is interesting and worth further investigation.

Remarkably, *in vitro* HDV infection was achieved not only in human HepG2 cells but also in cell lines originated from other tissues or species. These cell lines include HeLa, Vero, and CHO cells and in two mouse hepatocellular carcinoma cell lines, Hepa1-6 and MMHD3. Transfection of plasmid encoding hNTCP, mNTCP, or NTCP variants into these cells resulted in HBV pre-S1 lipopeptide binding in a pattern similar to that seen for HepG2 cells transfected with the same constructs. HDV can infect all of these cell lines complemented with hNTCP or mNTCP-h84-87, but not with mNTCP or hNTCP-m84-87, regardless of the species source of the cell lines or whether the cells originated from hepatocytes or not. These data indicate that the viral entry of HDV is probably not limited by other tissue- or species-specific host factors but by NTCP itself.

Unlike HDV, appreciable HBV infection could not be detected in hNTCP- or mNTCP-h84-87-transfected HeLa, Vero, CHO, Hepa1-6, and MMHD3 cells under the experimental conditions tested, indicating there may exist additional cellular factors, which may either facilitate or suppress HBV productive infection in culture at the entry or postentry level. Multiple cellular factors are frequently required for a productive viral infection at the entry level. For example, HIV entry is achieved by serial conformational changes of the trimeric glycoprotein GP160 upon sequential interactions with CD4, CCR5, or CXCR4, is also orchestrated with other cellular molecules, and is probably facilitated by clustering as a receptor complex for efficient infection (34, 35). HBV contains three surface proteins: L (large), M (medium), and S (small) envelope proteins. In addition to pre-S1 of L protein, which mediates specific NTCP receptor binding (11, 12), and the antigenic loop of the S domain, which has been demonstrated to mediate initial attachment of the virus to cell surface via HSPG (36, 37), it is possible that other regions of the envelope proteins may interact with yet-unidentified cellular factor(s) that may vary among individual cells, either species specific or not, and contribute considerably to the entry efficiency of HBV and to a smaller extent or differentially to HDV viral entry.

In addition to cellular (co)receptor and factor(s) for viral entry, postentry factors can profoundly influence tissue and host tropism. Tissue or cell type tropism of viral infection is sometimes restricted by cell-based antiviral defense mechanisms, for example, species specificity of primate lentiviruses imposed by the cytoplasmic body component TRIM5α (38) and the cytidine deaminase APOBEC3G (39), which blocks cross-species infection by targeting incoming viral capsid and deoxycytidines in reverse-transcribed viral cDNAs, respectively. Moreover, retroviral infection could also be restrained by molecules such as CD317, also known as tetherin (40, 41), which targets the progeny viral particle budding process. In fact, productive infection of HBV of human hepatocytes critically depends on some liver-specific transcription factors, e.g., HNF4A and HLF (42). APOBEC3 was shown to be a major cellular restriction factor(s) for HBV *in vitro* and *in vivo* (43–45). The undetectable HBV infection that we observed in cells other than HepG2-NTCP may also be attributable to the missing of liver-specific transcription factors or the present of postentry cellular restriction factor(s) presented in these cells. Further studies are therefore warranted to identify additional facilitating or suppressing cellular factor(s) for a productive HBV infection in these cells.

ACKNOWLEDGMENTS

This study was supported by the Major State Basic Research Development Program of China (2010CB530101 and 2011CB812501) and by the Science and Technology Bureau of the Beijing Municipal Government.

REFERENCES

1. **Ganem D, Prince AM.** 2004. Hepatitis B virus infection: natural history and clinical consequences. N. Engl. J. Med. **350:**1118–1129.
2. **Lavanchy D.** 2004. Hepatitis B virus epidemiology, disease burden, treatment, and current and emerging prevention and control measures. J. Viral Hepat. **11:**97–107.
3. **Chan HL, Sung JJ.** 2006. Hepatocellular carcinoma and hepatitis B virus. Semin. Liver Dis. **26:**153–161.
4. **Hughes SA, Wedemeyer H, Harrison PM.** 2011. Hepatitis delta virus. Lancet **378:**73–85.
5. **Nassal M.** 1996. Hepatitis B virus morphogenesis. Curr. Top. Microbiol. Immunol. **214:**297–337.
6. **Kuo MY, Goldberg J, Coates L, Mason W, Gerin J, Taylor J.** 1988. Molecular cloning of hepatitis delta virus RNA from an infected woodchuck liver: sequence, structure, and applications. J. Virol. **62:**1855–1861.

7. **Bonino F, Heermann KH, Rizzetto M, Gerlich WH.** 1986. Hepatitis delta virus: protein composition of delta antigen and its hepatitis B virus-derived envelope. J. Virol. **58:**945–950.
8. **Barrera A, Guerra B, Lee H, Lanford RE.** 2004. Analysis of host range phenotypes of primate hepadnaviruses by in vitro infections of hepatitis D virus pseudotypes. J. Virol. **78:**5233–5243.
9. **Sureau C.** 2006. The role of the HBV envelope proteins in the HDV replication cycle. Curr. Top. Microbiol. Immunol. **307:**113–131.
10. **Blanchet M, Sureau C.** 2007. Infectivity determinants of the hepatitis B virus pre-S domain are confined to the N-terminal 75 amino acid residues. J. Virol. **81:**5841–5849.
11. **Yan H, Zhong G, Xu G, He W, Jing Z, Gao Z, Huang Y, Qi Y, Peng B, Wang H, Fu L, Song M, Chen P, Gao W, Ren B, Sun Y, Cai T, Feng X, Sui J, Li W.** 2012. Sodium taurocholate cotransporting polypeptide is a functional receptor for human hepatitis B and D virus. eLife **1:**e00049. doi:10.7554/eLife.00049.
12. **Zhong G, Yan H, Wang H, He W, Jing Z, Qi Y, Fu L, Gao Z, Huang Y, Xu G, Feng X, Sui J, Li W.** 2013. Sodium taurocholate cotransporting polypeptide mediates woolly monkey hepatitis B virus infection of *Tupaia* hepatocytes. J. Virol. **87:**7176–7184.
13. **Hagenbuch B, Meier PJ.** 1994. Molecular cloning, chromosomal localization, and functional characterization of a human liver Na+/bile acid cotransporter. J. Clin. Invest. **93:**1326–1331.
14. **Stieger B.** 2011. The role of the sodium-taurocholate cotransporting polypeptide (NTCP) and of the bile salt export pump (BSEP) in physiology and pathophysiology of bile formation. Handb. Exp. Pharmacol. **201:**205–259.
15. **Ananthanarayanan M, Ng OC, Boyer JL, Suchy FJ.** 1994. Characterization of cloned rat liver Na^+-bile acid cotransporter using peptide and fusion protein antibodies. Am. J. Physiol. **267:**G637–G643.
16. **Stieger B, Hagenbuch B, Landmann L, Hochli M, Schroeder A, Meier PJ.** 1994. In situ localization of the hepatocytic Na^+/taurocholate cotransporting polypeptide in rat liver. Gastroenterology **107:**1781–1787.
17. **Barker LF, Maynard JE, Purcell RH, Hoofnagle JH, Berquist KR, London WT.** 1975. Viral hepatitis, type B, in experimental animals. Am. J. Med. Sci. **270:**189–195.
18. **Su JJ.** 1987. Experimental infection of human hepatitis B virus (HBV) in adult tree shrews. Zhonghua Bing Li Xue Za Zhi **16:**103–122. (In Chinese.)
19. **Walter E, Keist R, Niederost B, Pult I, Blum HE.** 1996. Hepatitis B virus infection of *Tupaia* hepatocytes in vitro and in vivo. Hepatology **24:**1–5.
20. **Glebe D, Aliakbari M, Krass P, Knoop EV, Valerius KP, Gerlich WH.** 2003. Pre-s1 antigen-dependent infection of *Tupaia* hepatocyte cultures with human hepatitis B virus. J. Virol. **77:**9511–9521.
21. **Guidotti LG, Matzke B, Schaller H, Chisari FV.** 1995. High-level hepatitis B virus replication in transgenic mice. J. Virol. **69:**6158–6169.
22. **Lucifora J, Vincent IE, Berthillon P, Dupinay T, Michelet M, Protzer U, Zoulim F, Durantel D, Trepo C, Chemin I.** 2010. Hepatitis B virus replication in primary macaque hepatocytes: crossing the species barrier toward a new small primate model. Hepatology **51:**1954–1960.
23. **Polo JM, Jeng KS, Lim B, Govindarajan S, Hofman F, Sanqiorqi F, Lai MM.** 1995. Transgenic mice support replication of hepatitis delta virus RNA in multiple tissues, particularly in skeletal muscle. J. Virol. **69:**4880–4887.
24. **Schieck A, Schulze A, Gahler C, Muller T, Haberkorn U, Alexandrov A, Urban S, Mier W.** Hepatitis B virus hepatotropism is mediated by specific receptor recognition in the liver and not restricted to susceptible hosts. Hepatology, in press. doi:10.1002/hep.26211.
25. **Meier A, Mehrle S, Weiss TS, Mier W, Urban S.** The myristoylated preS1-domain of the hepatitis B virus L-protein mediates specific binding to differentiated hepatocytes. Hepatology, in press. doi:10.1002/hep.26181.
26. **Petersen J, Dandri M, Mier W, Lutgehetmann M, Volz T, von Weizsacker F, Haberkorn U, Fischer L, Pollok JM, Erbes B, Seitz S, Urban S.** 2008. Prevention of hepatitis B virus infection in vivo by entry inhibitors derived from the large envelope protein. Nat. Biotechnol. **26:**335–341.
27. **Sureau C, Moriarty AM, Thornton GB, Lanford RE.** 1992. Production of infectious hepatitis delta virus in vitro and neutralization with antibodies directed against hepatitis B virus pre-S antigens. J. Virol. **66:**1241–1245.
28. **Blanchet M, Sureau C.** 2006. Analysis of the cytosolic domains of the hepatitis B virus envelope proteins for their function in viral particle assembly and infectivity. J. Virol. **80:**11935–11945.
29. **Van Dyke RW, Stephens JE, Scharschmidt BF.** 1982. Bile acid transport in cultured rat hepatocytes. Am. J. Physiol. **243:**G484–G492.
30. **Schieck A, Schulze A, Gahler C, Muller T, Haberkorn U, Alexandrov A, Urban S, Mier W.** 2013. Hepatitis B virus hepatotropism is mediated by specific receptor recognition in the liver and not restricted to susceptible hosts. Hepatology doi:10.1002/hep.26211.
31. **Hu NJ, Iwata S, Cameron AD, Drew D.** 2011. Crystal structure of a bacterial homologue of the bile acid sodium symporter ASBT. Nature **478:**408–411.
32. **Schulze A, Gripon P, Urban S.** 2007. Hepatitis B virus infection initiates with a large surface protein-dependent binding to heparan sulfate proteoglycans. Hepatology **46:**1759–1768.
33. **Leistner CM, Gruen-Bernhard S, Glebe D.** 2008. Role of glycosaminoglycans for binding and infection of hepatitis B virus. Cell Microbiol. **10:**122–133.
34. **Yi L, Fang J, Isik N, Chim J, Jin T.** 2006. HIV gp120-induced interaction between CD4 and CCR5 requires cholesterol-rich microenvironments revealed by live cell fluorescence resonance energy transfer imaging. J. Biol. Chem. **281:**35446–35453.
35. **Wilen CB, Tilton JC, Doms RW.** HIV: cell binding and entry. Cold Spring Harbor Perspect. Med., in press. doi: 10.1101/cshperspect.a006866.
36. **Sureau C, Salisse J.** 2013. A conformational heparan sulfate binding site essential to infectivity overlaps with the conserved hepatitis B virus a-determinant. Hepatology **57:**985–994.
37. **Salisse J, Sureau C.** 2009. A function essential to viral entry underlies the hepatitis B virus "a" determinant. J. Virol. **83:**9321–9328.
38. **Stremlau M, Owens CM, Perron MJ, Kiessling M, Autissier P, Sodroski J.** 2004. The cytoplasmic body component TRIM5α restricts HIV-1 infection in Old World monkeys. Nature **427:**848–853.
39. **Sheehy AM, Gaddis NC, Choi JD, Malim MH.** 2002. Isolation of a human gene that inhibits HIV-1 infection and is suppressed by the viral Vif protein. Nature **418:**646–650.
40. **Neil SJ, Zang T, Bieniasz PD.** 2008. Tetherin inhibits retrovirus release and is antagonized by HIV-1 Vpu. Nature **451:**425–430.
41. **Goffinet C, Schmidt S, Kern C, Oberbremer L, Keppler OT.** 2010. Endogenous CD317/tetherin limits replication of HIV-1 and murine leukemia virus in rodent cells and is resistant to antagonists from primate viruses. J. Virol. **84:**11374–11384.
42. **Moolla N, Kew M, Arbuthnot P.** 2002. Regulatory elements of hepatitis B virus transcription. J. Viral Hepat. **9:**323–331.
43. **Lei YC, Hao YH, Zhang ZM, Tian YJ, Wang BJ, Yang Y, Zhao XP, Lu MJ, Gong FL, Yang DL.** 2006. Inhibition of hepatitis B virus replication by APOBEC3G in vitro and in vivo. World J. Gastroenterol. **12:**4492–4497.
44. **Suspene R, Guetard D, Henry M, Sommer P, Wain-Hobson S, Vartanian JP.** 2005. Extensive editing of both hepatitis B virus DNA strands by APOBEC3 cytidine deaminases in vitro and in vivo. Proc. Natl. Acad. Sci. U. S. A. **102:**8321–8326.
45. **Vartanian JP, Henry M, Marchio A, Suspene R, Aynaud MM, Guetard D, Cervantes-Gonzalez M, Battiston C, Mazzaferro V, Pineau P, Dejean A, Wain-Hobson S.** 2010. Massive APOBEC3 editing of hepatitis B viral DNA in cirrhosis. PLoS Pathog. **6:**e1000928. doi:10.1371/journal.ppat.1000928.